



Achieving superior mechanical properties in friction lap joints of copper to carbon-fiber-reinforced plastic by tool offsetting

L.H. Wu*, K. Nagatsuka, K. Nakata

Joining and Welding Research Institute, Osaka University, 11-1, Mihogaoka, Ibaraki, Osaka, 567-0047, Japan

ARTICLE INFO

Article history:

Received 30 November 2017

Received in revised form 17 April 2018

Accepted 18 April 2018

Available online 22 April 2018

Keywords:

Hybrid joining

Plastic

Metal

Carbon-fiber-reinforced plastic

Properties

ABSTRACT

It is a challenge to achieve a sound welded metal/carbon-fiber-reinforced thermoplastic (CFRTP) joint with high strength and few bubbles. In this study, sound lap joints of Cu and CFRTP were obtained by friction lap joining (FLJ) directly at rotation rates of 600–2000 rpm, with the welding tool at the joint center and offsetting the tool 7 mm away from the center toward the retreating side, respectively. Tool offsetting reduced the non-uniform temperature distribution in the lap joints resulting from the high conductivity of Cu, which not only enhanced the tensile shear force from 0.89–2.25 kN to 1.71–3.54 kN, with the maximum increasing rate of 135%, but also reduced the bubble area to only 19% of the original level of 2000 rpm. It is the first time to report a high-quality Cu/CFRTP joint with a high strength and few bubbles. The large increase of the strength after tool offsetting was attributed to the increase of the joining area, the decrease of bubbles and the decrease of the CFRTP degradation. The details on the generation, quantitative distribution and expulsion of the bubbles in the FLJ joints were discussed.

© 2018 Published by Elsevier Ltd on behalf of The editorial office of Journal of Materials Science & Technology.

1. Introduction

The hybrid joining of metals to plastic-based materials, including carbon-fiber reinforced thermoplastic (CFRTP), is increasingly demanded in various industries to achieve the flexible and lightweight design of the parts. It is because the hybrid joints could combine the advantages of metals and plastic-based materials, such as the superior thermal and electrical conductivity for metals and the light-weight and good corrosion resistance for plastic-based materials. However, the direct joining of metals to plastic-based materials is not easy since there are large differences in the physical and chemical properties.

Conventionally, adhesive bonding [1] and mechanical fastening [2] are the commonly used methods for the joining of metals to plastic-based materials. However, there are some shortcomings for these two conventional joining methods. For adhesive bonding, it not only produces environmental pollutants and is a time-consuming process, but also, it is very susceptible to degradation due to the environmental factors [1,3]. Mechanical fastening usually leads to a stress concentration and non-flexible structural design. To solve these problems, novel welding methods such as

laser welding [4,5], friction stir spot welding [6] and ultrasonic welding [7] have recently been applied in the joining of metals to plastic-based materials.

Several investigators [4,8–11] have reported on the joining of plastic-based materials with metals including Al, Mg and steel utilizing lasers as the heat source, and found that plastic-based materials could join well with metals by laser welding. Katayama and coworkers [4,9–11] suggested that the plastic-based materials joined with metals mainly because of chemical or physical bond between plastics and oxide on metals' surface, as well as mechanical interlocking effect. Besides, they suggested that the bubbles were mainly generated by the thermal decomposition of plastics, which were benefit for the bonding of plastics and metals during joining, because the great pressure due to the expansion of bubbles pushed the melted plastic to bond with the metals.

However, bubbles are very difficult to expel from the joint due to a low applied stress in the laser-welded joints. As a result, the large fraction of bubbles inevitably remains in the laser-welded joints. They would be harmful to the properties of the joint, especially for the tensile and fatigue properties, because the bubbles seldom have load-bearing ability, and a stress concentration probably occurs around the bubbles during a tensile test and cyclic loading [12]. Also, from the industry application viewpoint, the joints with a high level of bubbles are not allowed. Moreover, laser welding has its own questions, such as the high cost of laser power and com-

* Corresponding author.

E-mail address: lhwu@imr.ac.cn (L.H. Wu).

plex welding parameters. At present, laser welding of plastics to metals is still in the developing stage, and thus more deep studies need to be made to solve the problems above. It was also reported that sound joints of plastic-based materials with metals could be obtained by friction stir spot welding [6] and ultrasonic welding [13]. However, these joining methods are usually viable for limited joint geometries and dimensions, which limit their application.

Friction lap joining (FLJ), a new variation of friction stir welding (FSW), has been widely studied for Al, Mg, and Ti alloys [14,15], and has recently been applied to the lap joining of metals to plastic-based materials [3,16]. The principle of FLJ is based on that of FSW, but the difference is that the FLJ tool just consists of a shoulder without a pin, and thus no “stirring” effect occurs. The basic FLJ principle for metals and plastic-based materials is as follows. During FLJ, the heat, originating from the friction of the welding tool and metals, is conducted into the plastic-based materials, causing the plastics to be melted and thermally decomposed. Under the pressure of the tool, the softened metals and melted plastics are pushed into each other for bonding, and after the melted plastics are re-solidified, the plastic-based materials can join with the metals.

It was reported that FLJ could successfully join plastic-based materials to Al, Mg and steel [3,12,16,17]. Liu et al. [12] found that the volume of bubbles in the joints affected the joint strength, and a strong FLJ joint with an area fraction of bubbles <8% was obtained after welding process optimization. Moreover, Nagasaki et al. [3] found that a hydrogen bond between the amide function group of polyamide-based plastics and oxide on the surface of the metals played an important role in the joining of CFRTP with metals. Besides, the joint strength could be largely increased via the silane coupling pretreatment on Al alloy surface before FLJ, which showed almost the same strength with that of base CFRTP material, fracturing at the base CFRTP material [3,18].

Many investigations have indicated that the novel joining methods above can join plastic-based materials well with metals [3–7]. However, the metals for joining focused on Al, Mg and steel. At present, the reports on the joining of plastic-based materials with Cu are very limited and preliminary. The limited report [19] indicated that it was not easy to obtain a strong Cu-plastic joint by laser welding, and to obtain a defect-free joint required a large quantity of energy input, as the result of the high reflectivity for the laser and high thermal conductivity of Cu. More recently, the present authors [20] reported the feasibility of the FLJ of CFRTP to Cu. It was found that CFRTP could directly join to Cu by FLJ without any adhesives or chemical treatment, showing an advantage over laser welding, where FLJ could obtain a relatively strong CFRTP-Cu joint (2.3 kN for tensile shear force, 15 mm wide, and 10.2 MPa for nominal tensile shear strength) with a relative low heat input. However, this joint strength was still not high enough.

In addition, a large fraction of bubbles was still found in these FLJ joints [20]. During the FLJ of plastic-based materials to metals, the welding temperatures are usually over 400 °C [3,20]. Thus, plastics with a low temperature for thermal decomposition, such as

polyamide 6 (PA6, 350 °C for thermal decomposition), are usually degraded to generate bubbles during FLJ. Although the downforce of the welding tool could expel some bubbles, they still inevitably remain in the joints after joining. It was reported that the distribution, number and size of bubbles, which were closely related with the FLJ processing parameters, largely affected the joint properties [12]. Thus, it is of great significance to study the relationship between the distribution, number and size of bubbles and FLJ parameters, and how to adjust FLJ parameters to control these factors to reduce the bubbles as many as possible, and finally enhance the strength and quality of the joints.

In this study, CFRTP (PA6 matrix) was joined to Cu by FLJ with the tool located at the joint center and offsetting the tool away from the center, respectively, at rotation rates of 600–2000 rpm, with a constant travel speed of 600 mm/min. The aim was to (a) determine the effect of rotation rate on the joint characters and strength, (b) clarify whether tool offsetting could improve the quality and strength of the joints and (c) understand the characteristics of the bubbles in the joints at different rotation rates and tool positions, and thus to obtain CFRTP-Cu joints of high strength with a low level of bubbles.

2. Materials and methods

The as-received materials were 3-mm-thick CFRTP sheets (PA6 matrix with 20 wt.% carbon fiber addition) made by injection molding, and 2-mm-thick oxygen-free Cu sheets. The average tensile strengths of the CFRTP were 140 MPa in the flow direction and 117 MPa in the transverse direction. For more details on the CFRTP, please refer to the previous work [3]. Before FLJ, the Cu sheets were ground in flowing water with #800 emery paper, and CFRTP sheets were dry-ground with #80 and #800 emery paper. The CFRTP sheets were friction lap joined to Cu at rotation rates of 600–2000 rpm with a constant joining speed of 600 mm/min. A tool plunge depth of 0.9 mm, a tilt angle of 3°, and an overlap width of 30 mm were used by a steel tool. The welding tool just consisted of a flat shoulder 15 mm in diameter without a pin.

In this study, the welding tool during FLJ was placed in two different positions of the overlap zone. A schematic of the joining process, with the temperature measurement positions, is shown in Fig. 1. The welding tool was placed in the center of the overlap zone (Fig. 1a), and was offset 7 mm away from the center toward the edge of the overlap zone on the retreating side (RS), i.e. the Cu side (Fig. 1b). For simplification, these joining processes will be called the normal FLJ and offset FLJ, respectively, in the following sections. For the temperature measurement during normal FLJ, K-type thermocouples were inserted at the Cu sheet/CFRTP sheet interface in the four locations: at the center of the overlap zone, from the center line away 7.5 mm on the RS and advancing side (AS), and from the center line away 15 mm on the RS, i.e. the very edge of the lapped zone on the RS, which were marked as Points C, R, A and E in Fig. 1a. For comparison, at 1500 rpm, 600 mm/min during offset FLJ, K-type thermocouples were also inserted at Cu sheet/CFRTP sheet inter-

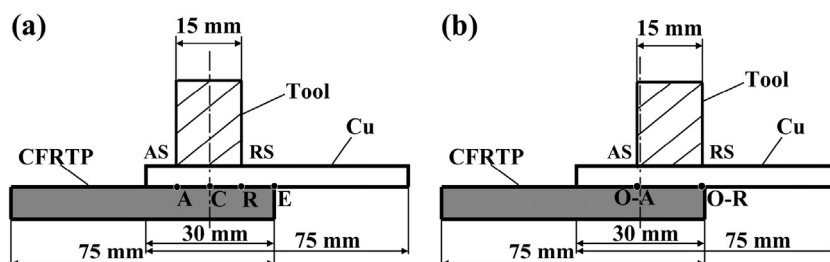


Fig. 1. Schematic illustration of Cu and CFRTP joining during (a) normal FLJ with the tool at the center line of overlap zone, and (b) offset FLJ with tool offsetting 7 mm from center line toward the RS. Temperature measuring positions of A, C, R and E during normal FLJ, and O-A and O-R during offset FLJ are marked in (a) and (b), respectively.

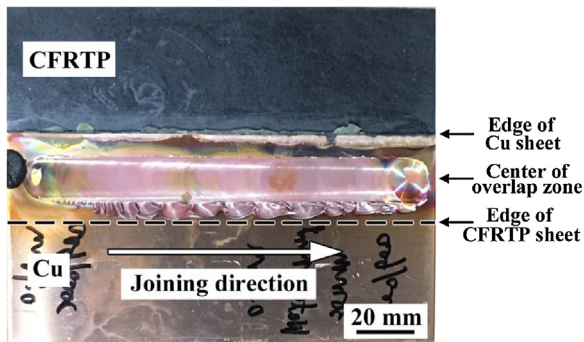


Fig. 2. Typical macrostructural morphology of normal friction lap joint of Cu/CFRTP at 2000 rpm with tool located at center of overlap zone.

face 7.5 mm away from the offset tool center on the RS and AS. These were marked as Points O-R and O-A, respectively, in Fig. 1b.

The specimens for microstructural observation were first cut perpendicular to the joining direction, and then ground and polished with a silica solution. The microstructural observation of these specimens was then performed via optical microscopy (OM) and scanning electron microscopy (SEM). To test the tensile shear force (TSF), specimens were cut perpendicular to the joining direction with a width of 15 mm. The Vickers hardness measurement was made using 50 gf and holding for 15 s. Tensile shear tests were carried out in a regular tensile machine at the crosshead speed of 0.5 mm/min. For each joining condition, three tensile specimens were tested, and in order to reduce the effect of travel position on the microstructure and mechanical properties, the specimens were all cut from the travel distance of 60–120 mm. The fracture surfaces of the tensile shear specimens were observed using OM and SEM.

The residual CFRTP areas on the fractured surface of Cu were measured manually using Photoshop software. The number and size of bubbles in the joints, which were observed from both fracture CFRTP surfaces and cross sections, were measured manually using Photoshop software. For the bubbles measured from the fracture surfaces, 16 random regions with an area of 1.13 mm² (100 × in SEM images) and almost uniformly distributed across the fracture surface of each joint, were chosen for statistical analysis. All of the bubbles in the cross sections were measured.

3. Results and discussion

3.1. Asymmetric fracture surface characteristics and welding temperature for normal FLJ joints

After normal FLJ, CFRTP could be joined well to Cu at all the rotation rates of 600–2000 rpm, and all of the joints could not be separated by human hand force. The typical surface of the Cu/CFRTP

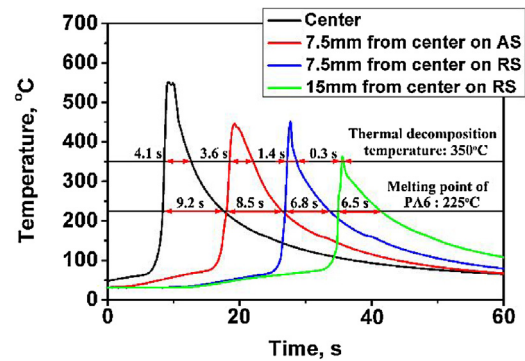


Fig. 4. Temperature measurements at different positions of normal FLJ CFRTP-Cu joint at 1500 rpm. Black, red, blue and green curves stand for the temperature on points C, A, R and E, respectively in Figs. 1a and Fig. 3.

joint at 2000 rpm is shown in Fig. 2. After a tensile shear test of the joints, the normal FLJ joints at all the rotation rates fractured at the Cu/CFRTP interface. The typical fracture surface morphologies of CFRTP-Cu joints at 800, 1500 and 2000 rpm are shown in Fig. 3. It is clear that the fracture surfaces on Cu side included an area stick with residual CFRTP (surrounded by black dot line, known as the joining area) and another baked Cu area. As the rotation rate increased, the joining area increased. An interesting phenomenon is that the joining area on the AS and RS was asymmetric, and the residual CFRTP was obviously distributed toward the AS. In other words, the joining area on the AS was more than that on the RS. Besides, at 2000 rpm, there were some yellow re-solidified plastic. This yellow plastic was the result of the base plastic being over-decomposed, which had much less load bearing ability than the base plastic [21], and thus was not good for the joint strength.

In order to clarify the cause of the asymmetry of the joining area on the RS and AS, the temperature profile at different positions of the normal FLJ joint at 1500 rpm was measured, as shown in Fig. 4. At various positions across the overlap zone, the maximum temperature all exceeded the thermal decomposition and melting temperature of PA6, which suggested that the PA6 across the lapped zone had melted. In addition, the temperature curves 7.5 mm away from the joint center on the RS (blue curve) and the AS (red curve) were different, and the cooling rate on the RS was much faster than that on the AS. The staying time above the melting point and decomposition temperature was about 8.5 s and 3.6 s, respectively on the AS, while only about 6.8 s and 1.4 s on the RS. This can be explained by the high thermal conductivity of Cu.

As we know, the thermal conductivity of Cu was about 401 W/(mK) [22]. At such a high thermal conductivity, the heat in the joint (the tool center was regarded as the heat source) would be conducted quickly into the near Cu sheet with lower tempera-

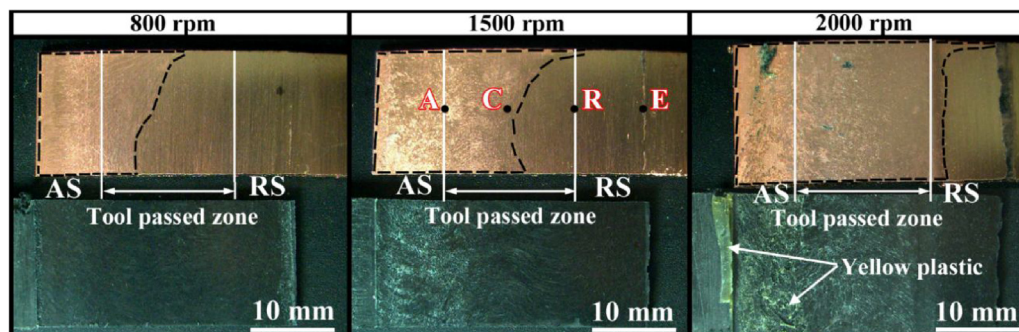


Fig. 3. Typical macrostructures of the opposing fractured surfaces of normal joints at 800, 1500 and 2000 rpm. Points of A, C, R and E on the fracture surface at 1500 rpm correspond to the positions for temperature measurement in Fig. 1.

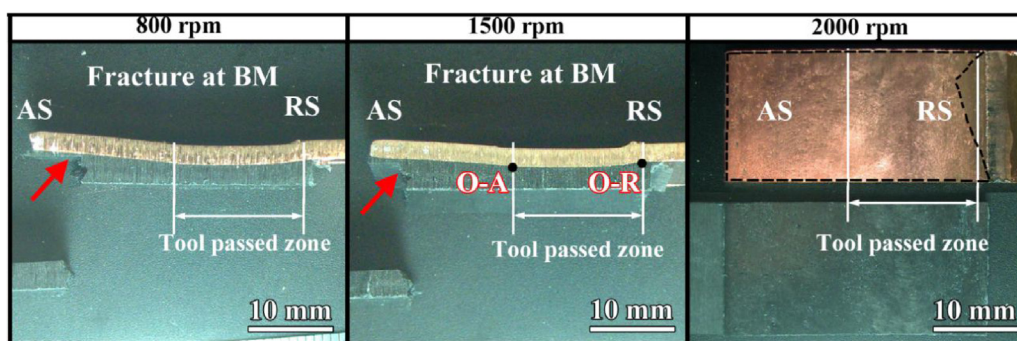


Fig. 5. Typical macrostructures of the opposing fractured surfaces of offset joints at 800, 1500 and 2000 rpm. The points of O-A and O-R on the fracture surface at 1500 rpm were the positions used for temperature measurement.

ture. The width of the whole Cu sheet was 75 mm, and the overlap width was only 30 mm. It means that the width of Cu sheet for heat conduction on the AS (15 mm) was much less than that on the RS (60 mm). Thus, the materials on the RS would rapidly cool down below the melting temperature of PA6. It was reported that the main joining mechanism of Cu to CF RTP was attributed to the formation of hydrogen bond between the Cu_2O on the Cu surface and amide group (CONH) of PA6 [20]. On the RS, there was not enough time for the formation of hydrogen bonding resulting from the short duration at high temperature (Fig. 4). It would explain why the joining area was much more on the AS.

3.2. Mechanical properties and fracture surface characteristics after tool offsetting

As is mentioned above, too fast cooling rate was the main cause of no bonding on the RS. In order to increase the whole joining area, we reduced the cooling rate on the RS by offsetting the welding tool 7 mm away from the joint center toward the RS (Fig. 1b). After tool offsetting, the fracture modes changed for 800–1500 rpm where the joints fractured at the CF RTP base material, although the fracture still occurred at the CF RTP–Cu interface at 600 and 2000 rpm. The typical fracture morphologies are shown in Fig. 5. After tool offsetting, the joining area obviously increased (Figs. 3 and 5). For 2000 rpm, the yellow plastic was hardly observed and the residual CF RTP was distributed uniformly on the Cu surface, which suggested that the degradation of CF RTP probably decreased after tool offsetting.

The variation of the TSF with the rotation rate for the normal and offset joints is shown in Fig. 6a. For both normal and offset joints, as the rotation rate increased, the TSF showed an increasing trend first, and then decreased. The maximum TSF achieved at 1500 rpm. Tool offsetting enhanced the joint TSF at each parameter, from 0.89–2.25 kN to 1.71–3.54 kN. The estimated residual CF RTP areas (i.e. joining area) on the Cu surfaces for the joints are shown in Fig. 6b. After tool offsetting, the joining area increased for every rotation rate except at 600 rpm. Therefore, tool offsetting could increase both the TSF and the joining area.

The typical temperature measurement at the edge of the tool on the RS and AS (point O-R and O-A, respectively, in Figs. 1b and 5) during offset FLJ at 1500 rpm is shown in Fig. 6c. The duration above the melting and thermal decomposition temperature on the RS was about 8.4 s and 1.8 s, and 9.3 s and 1.6 s on the AS, respectively. Compared to that for the normal joint (Fig. 4), the material of the offset joint showed a longer duration at high temperature on the RS while a shorter duration over the thermal decomposition temperature on the AS. This is because after tool offsetting, the width for heat conduction from the tool center increased on the AS but decreased on the RS (Fig. 1). Therefore, the increase of the joining area for the offset joints should be mainly attributed

to the decrease of the cooling rate on the RS, and thus there was enough time to form hydrogen bond between PA6 and Cu_2O on the Cu surface.

Fig. 6d shows the increasing efficiency of the TSF and the estimated residual CF RTP area after tool offsetting. At 800 and 1000 rpm, the increasing efficiency of the TSF was very close to that of the joining area. However, at other parameters, there was some difference between them. For example, at 2000 rpm, the increasing efficiency was even reached 135%, while the increasing efficiency of joining area was just 8.1%. At 600 rpm, the joining area decreased but the TSF increased after tool offsetting. In our previous paper [19], we have suggested that the joining area, the bubbles and the CF RTP degradation were the main factors influencing the joint TSF. Therefore, according to the relationship of the increasing efficiency of the TSF and the joining area, the increasing of the TSF at 800 and 1000 rpm should be mainly attributed to the increase of the joining area. While for other parameters especially for 600 and 2000 rpm, the bubbles and the CF RTP degradation should also contribute a lot to the increase of the TSF. Therefore, besides the joining area analyzed above, we will analyze the cause of the increase of the joint TSF from another two factors: the bubbles and the CF RTP degradation, which will be exhibited in Sections 3.3 and 3.4, respectively.

3.3. Bubbles formation and distribution in the FLJ joints

The macrostructural cross sections of the normal and offset joints are shown in Fig. 7. The interface of each joint showed a concave shape, whose curvature, depending on the melting and softening extent of CF RTP, increased with the rotation rate. A zone consisting of white dots was observed in the CF RTP near the interface of each joint, which corresponded to the re-solidified layer. These white dots were bubbles described in the following section. As the rotation rate increased, the re-solidified layer with the bubbles became thicker. It was reported that either the increase of the peak welding temperature or the duration at high temperature resulted in the increase of melted plastics and bubbles. During FLJ, with the rotation rate increasing, the peak welding temperature increased but the duration at high temperature did not increase remarkably [12]. Therefore, thicker re-solidified layer with more bubbles should be mainly related to higher peak temperature for the higher rotation rate.

The bubbles remaining in the joints were actually the combination result of the thermal decomposition of PA6 and being expelled. In this study, FLJ for different plunge depths of 0.3–0.9 mm at 2000 rpm were carried out to describe the generation and expulsion processes of bubbles (Fig. 8). For the normal joints, it was observed that as the plunge depth increased, the bubbles remaining in the joint increased (Fig. 8a, c and e). For the offset joints, the bubbles largely decreased, and only a few small bubbles remaining in the joints for all the plunge depths (Fig. 8b, d and f). As is mentioned

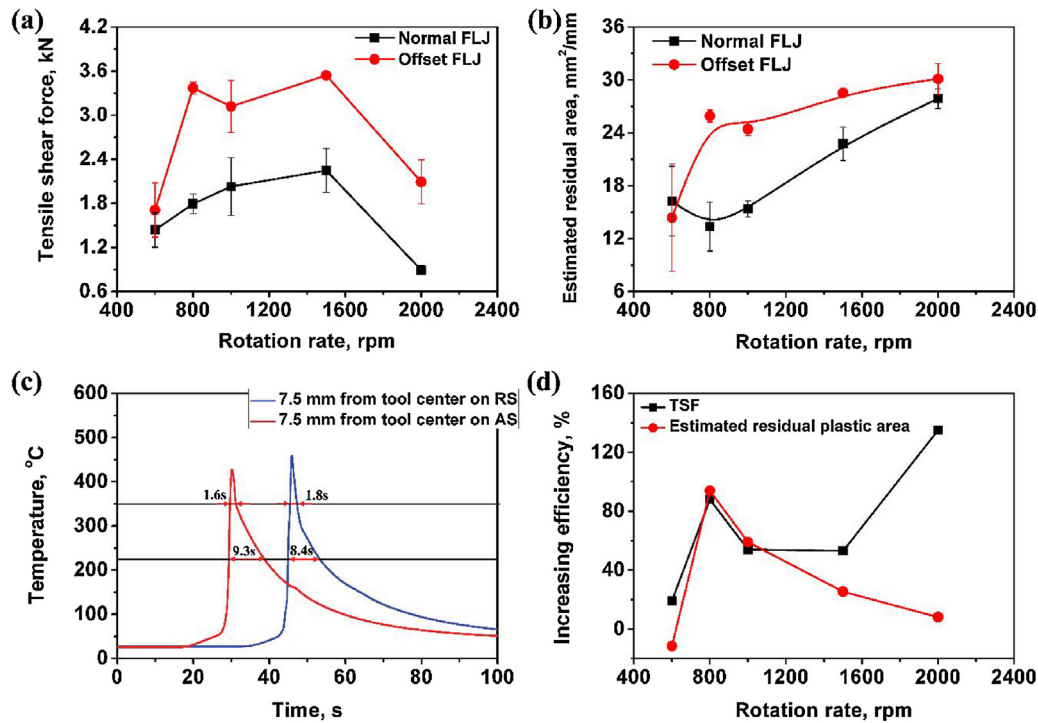


Fig. 6. (a) Variation of TSF with rotation rate for the normal and offset FLJ joints, (b) estimated residual CF RTP area on Cu surface for the normal and offset FLJ joints, (c) temperature measurement at edge of tool on AS and RS (Points O-A and O-R in Figs. 1b and 5) for offset FLJ joint at 1500 rpm, and (d) the increasing efficiency of TSF and residual CF RTP area for offset FLJ joint.

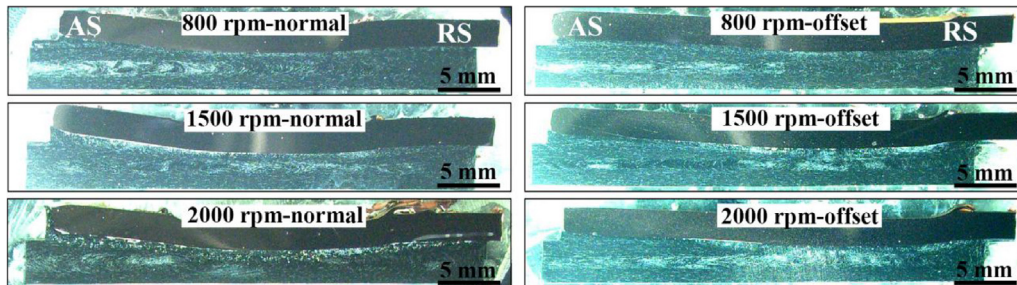


Fig. 7. Macrostructural cross sections of normal and offset Cu/CF RTP joints at different rotation rates.

above, welding temperature and the duration at high temperature is the main factors influencing the generation of bubbles. For the same parameter for normal and offset joints, the heat input and peak welding temperature should be similar. Therefore, fewer bubbles after tool offsetting might be mainly attributed to the decrease of the duration at high temperature (Figs. 4 and 6c).

According to Fig. 8, for the normal joints, at the plunge depths of 0.3 mm, only a few bubbles was observed at the edge of the joint (Fig. 8a). At 0.6 mm, the number of the bubbles increased, and most of them located at 130–420 μm away from the edge (Fig. 8c), with some bubbles observed in the expelled plastic out of the joint (also called “flash”, insert of Fig. 8c). For further plunge of 0.9 mm, a large number of bubbles remained across the joint from the center to the edge, and the typical bubbles in the center are shown in Fig. 8e. It suggested that when the heat input was low, bubbles could be almost expelled out. But when the heat input increased, too many bubbles generated, and they could not be thoroughly expelled out. It means that the bubbles remaining in the joint were largely dependent of the heat input.

Therefore, the generation and expulsion process of the bubbles can be described as follows. After the tool plunged into the Cu sheet, the PA6 in the some specific region (we called it as Region A) melted,

which, under the downforce of the tool, flowed out along the gap between Cu sheet and CF RTP plate. As the heat input increased, bubbles were generated from the thermal decomposition of PA6 in the Region A. Some of these bubbles, accompanying with the flowing of the melted PA6, would flow out of the joint or into other regions of the joint. If the cooling rate was not too fast, those melted PA6 coming from Region A would be further thermally decomposed to generate more bubbles. During the whole joining process, the generation and expulsion processes described above repeated, which determined the final volume of bubbles in the joint. Therefore, the bubbles remaining in some specific region depended on three parts: 1. generation of bubbles in this area, largely depending on the heat input and cooling rate; 2. flowing in of bubbles, largely depending on downforce of the tool and the cooling rate; and 3. expulsion of bubbles, largely depending on downforce of the tool. In all, the bubbles remaining in the joint largely depended on the heat input, but the downforce of the tool and cooling rate of the joints also affected their volume.

Measuring the size and number from the fracture surface of the CF RTP side was a good way to quantify the bubble distribution in the Cu/CF RTP joints. Unfortunately, the offset joints at 800–1500 rpm fractured along the base CF RTP materials, and the bubbles could

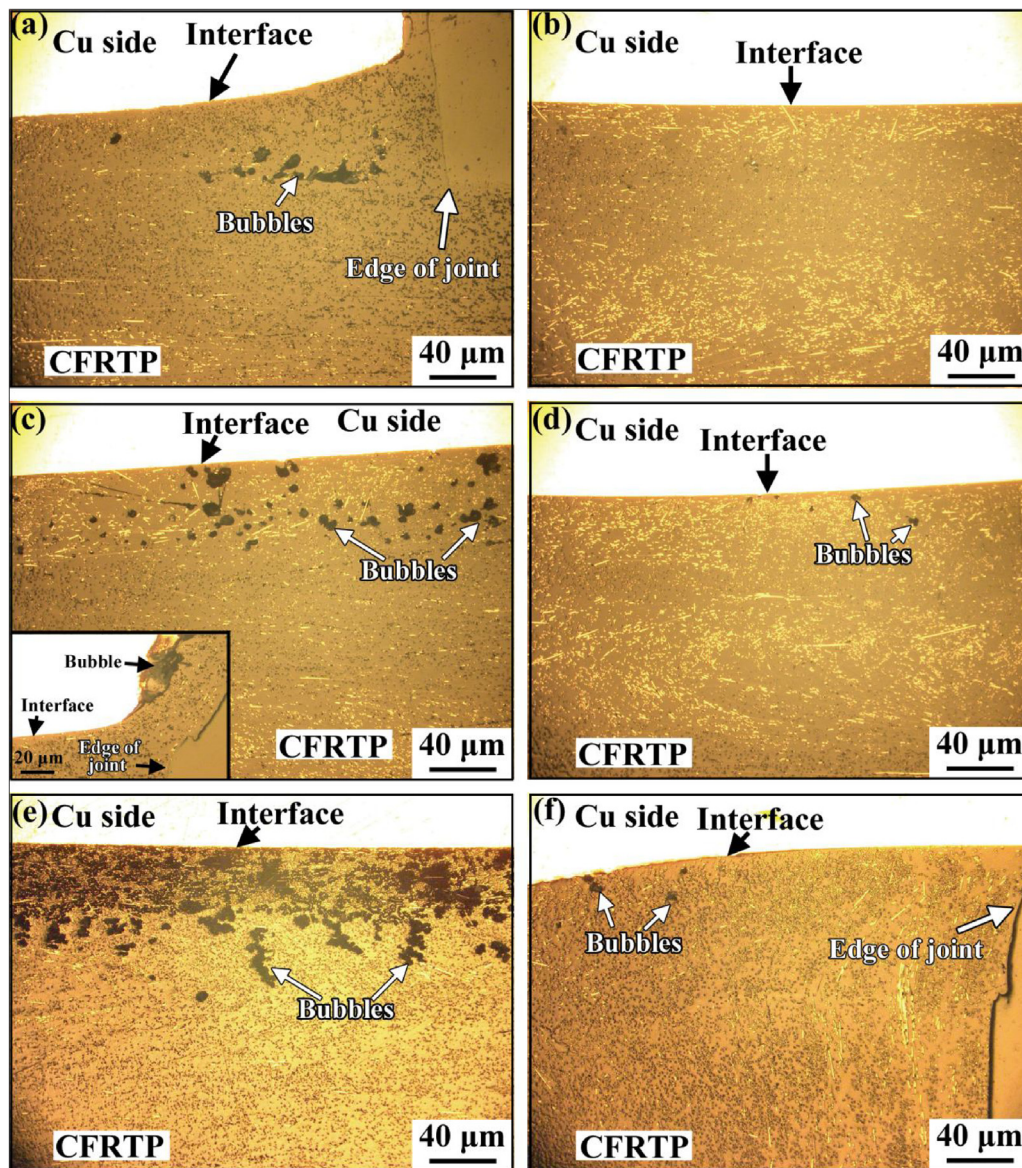


Fig. 8. Typical microstructure of Cu/CFRTP joints at 2000 rpm with different plunge depth for normal joints of (a) (c) (e) and for offset joints of (b) (d) (f): (a) (b) 0.3 mm, (c) (d) 0.6 mm, with (c) joint at edge inserted, and (e) (f) 0.9 mm.

not be measured from the fracture surface. In order to obtain the good statistical results, the bubbles were measured from both the observation of fracture surfaces and cross sections. Compared to the normal joints at all the rotation rates, the fraction and number of bubbles for offset joints obviously decreased, and the typical cross-sectional microstructures at 1500 rpm and microstructures for fracture surfaces at 2000 rpm are shown in Fig. 9.

Fig. 10 shows the distribution of the bubble area and number for both normal and offset joints. For the normal joints at 600 rpm and 2000 rpm (Figs. 10a and c), a large number of bubbles including large bubbles with the area $>0.5 \text{ mm}^2$ was observed. Tool offsetting largely reduced the area and number of bubbles (Figs. 10b and d), especially making those large bubbles disappear. For example, after tool offsetting, at 600 rpm, the bubble with the size $>0.003 \text{ mm}^2$ completely disappeared (Fig. 10b); at 2000 rpm, the large bubbles $>0.01 \text{ mm}^2$ largely decreased and the super large bubbles $>0.3 \text{ mm}^2$ disappeared (Figs. 10c, d and the inserts). At 1500 rpm, the areas of bubbles for both normal and offset joints were very small (most bubbles $<0.004 \text{ mm}^2$), and tool offsetting mainly reduced the number of the bubbles (Figs. 10e and f). It is well-known that the large

bubbles in the joints might have acted as the fracture sites, decreasing the strength of the joints. Therefore, tool offsetting reduced the chance of the large bubbles acting as the fracture sites, which was one of the reasons for increasing of the joint TSF.

Table 1 shows the statistical results of the bubbles measured from the fracture surface of the CFRTP sides. For the normal joints, as the rotation rate increased, the number and total area of bubbles decreased first, and then increased. At medium rotation rate (e.g. 1000 and 1500 rpm), the total area, fraction and average area of bubbles was small, which corresponded to a relatively high joint strength (Fig. 6a). It should be noted that at 1500 rpm, the number of the bubbles was the most and the average size of the bubbles was the least, while the TSF was largest within the normal FLJ joints (Fig. 6a). It suggests that those small bubbles might influence the joint strength very little, which agreed with the conclusion during laser welding of plastics to metals [10]. At 600 rpm, the total bubble area and the fraction of bubbles were largest, which can be explained by the formation and expulsion process. At 600 rpm, the volume of bubbles generated was small, but not enough heat and pressure to expel these bubbles, which resulted in the gathering of

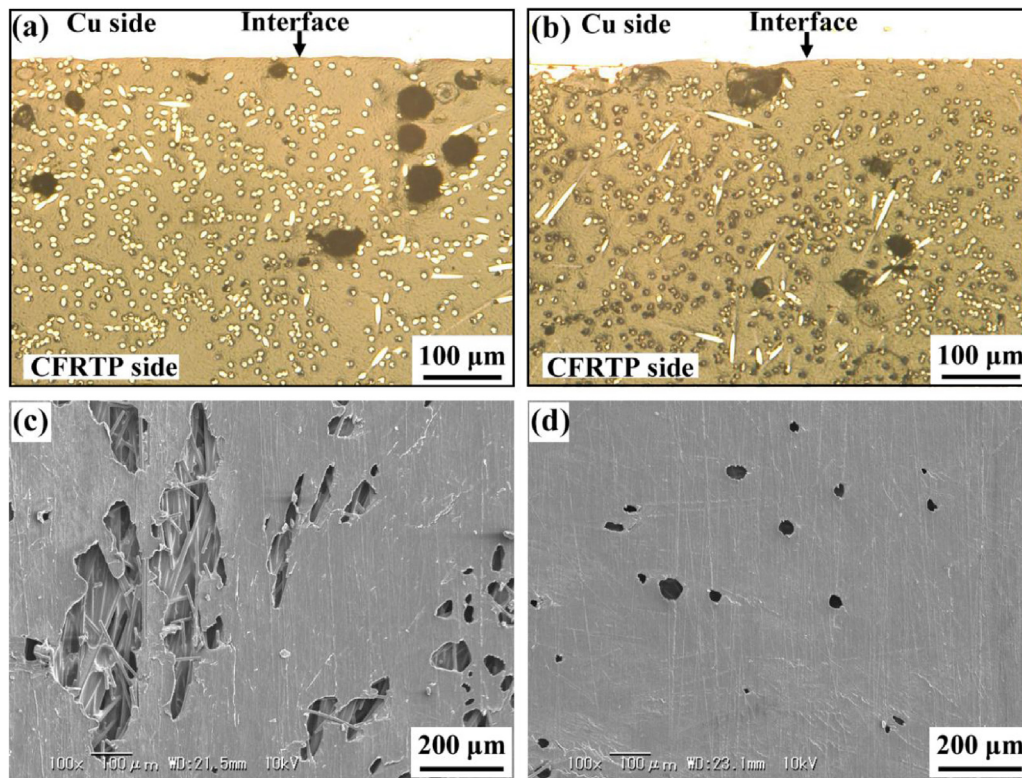


Fig. 9. Bubble comparison of joints for (a)(c) normal FLJ and (b)(d) offset FLJ: typical cross-section of FLJ Cu/CFRTP joint with (a) normal and (b) offset joints for 1500 rpm, fracture surfaces on the CFRTP side of (c) normal and (d) offset joints for 2000 rpm.

Table 1

Bubble statistical results for the normal and offset joints measured from fractured CFRTP surface.

| | Rotation rate, rpm | Number | Total area, mm ² | Fraction, % | Average size, mm ² | Bubble Area on AS, mm ² | Bubble Area on RS, mm ² |
|------------|--------------------|--------|-----------------------------|-------------|-------------------------------|------------------------------------|------------------------------------|
| Normal FLJ | 600 | 839 | 18.97 | 34.80 | 0.0226 | 17.64 | 1.33 |
| | 800 | 221 | 3.19 | 5.85 | 0.0144 | 3.08 | 0.11 |
| | 1000 | 531 | 1.90 | 3.48 | 0.0036 | 1.85 | 0.05 |
| | 1500 | 2800 | 3.19 | 5.84 | 0.0011 | 2.97 | 0.22 |
| | 2000 | 605 | 16.33 | 29.95 | 0.0270 | 13.93 | 2.40 |
| Offset FLJ | 600 | 15 | 0.015 | 0.027 | 0.0010 | 0 | 0.015 |
| | 2000 | 516 | 3.06 | 5.57 | 0.0059 | 1.77 | 1.29 |

many bubbles into huge bubbles at the edge (super large bubbles in Fig. 10a).

The bubbles on the AS were much more than that on the RS (Table 1). It could be explained by the difference of the cooling rate on two sides (Fig. 4). As is mentioned above, the bubbles remaining in specific region depended on three parts. Compared to that on the RS, because of smaller cooling rate on the AS (Fig. 4), more melted plastics accompanied by more bubbles flowed into this area, and a long heating time above the thermal decomposition would accelerate the degradation of plastics to generate more bubbles. Therefore, the bubbles mainly distributed on the AS for normal joints. Besides, at 600 and 2000 rpm, the fraction of the bubbles was over or approached to 30%. After tool offsetting, it reduced into less than 6% (Table 1), and the total area of bubbles reduced into only 0.1% and 19% of the original level at 600 rpm and 2000 rpm, respectively. It was attributed to the fact that tool offsetting largely reduced the bubbles with large size (Figs. 10a–d).

Table 2 shows the results of the bubble measured from the joint cross sections. For normal joints, the trend for the number and total area of the bubbles with rotation rate was similar to that observed from the fracture surface (Table 1). The total area of the bubbles decreased for each rotation rate after tool offsetting. For example, at 800 rpm, the total area of the bubbles was only 0.02 mm², only

33% of the original level after tool offsetting. Especially at 2000 rpm, the total area of the bubbles reduced from 10.7 mm² into only 0.15 mm², and the average size reduced to less than 1/10 of the original average size. Combining the TSF and the bubble statistics (Figs. 6a, d and Tables 1, 2), it was found that tool offsetting not only enhanced the TSF from 0.89–2.25 kN to 1.71–3.54 kN, with the maximum increasing rate of 135%, but also reduced the bubble area to only 19% of the original level at 2000 rpm. For the offset joint at 800 rpm, the area of the bubbles was only 0.02 mm², with a high TSF of 3.37 kN. Therefore, tool offsetting is a good method to achieve a high joint strength with few bubbles for the FLJ of Cu to CFRTP.

3.4. The CFRTP degradation and vickers hardness of FLJ joints

Fig. 11 shows the Vickers hardness of the CFRTP side in the normal and offset Cu/CFRTP joints at 2000 rpm. Compared to the normal joints, the offset joints showed a more uniform hardness distribution. For the normal joint, a high hardness zone exhibited near the tool center line, while near the edge of the joint on the AS, there was low hardness zone. As we know, during FLJ, the matrix (PA6) of CFRTP in the center would melt and flow out. But the carbon fibers in the CFRTP did not flow as well as melted PA6, and thus they would remain in the center after the melted PA6 flowed

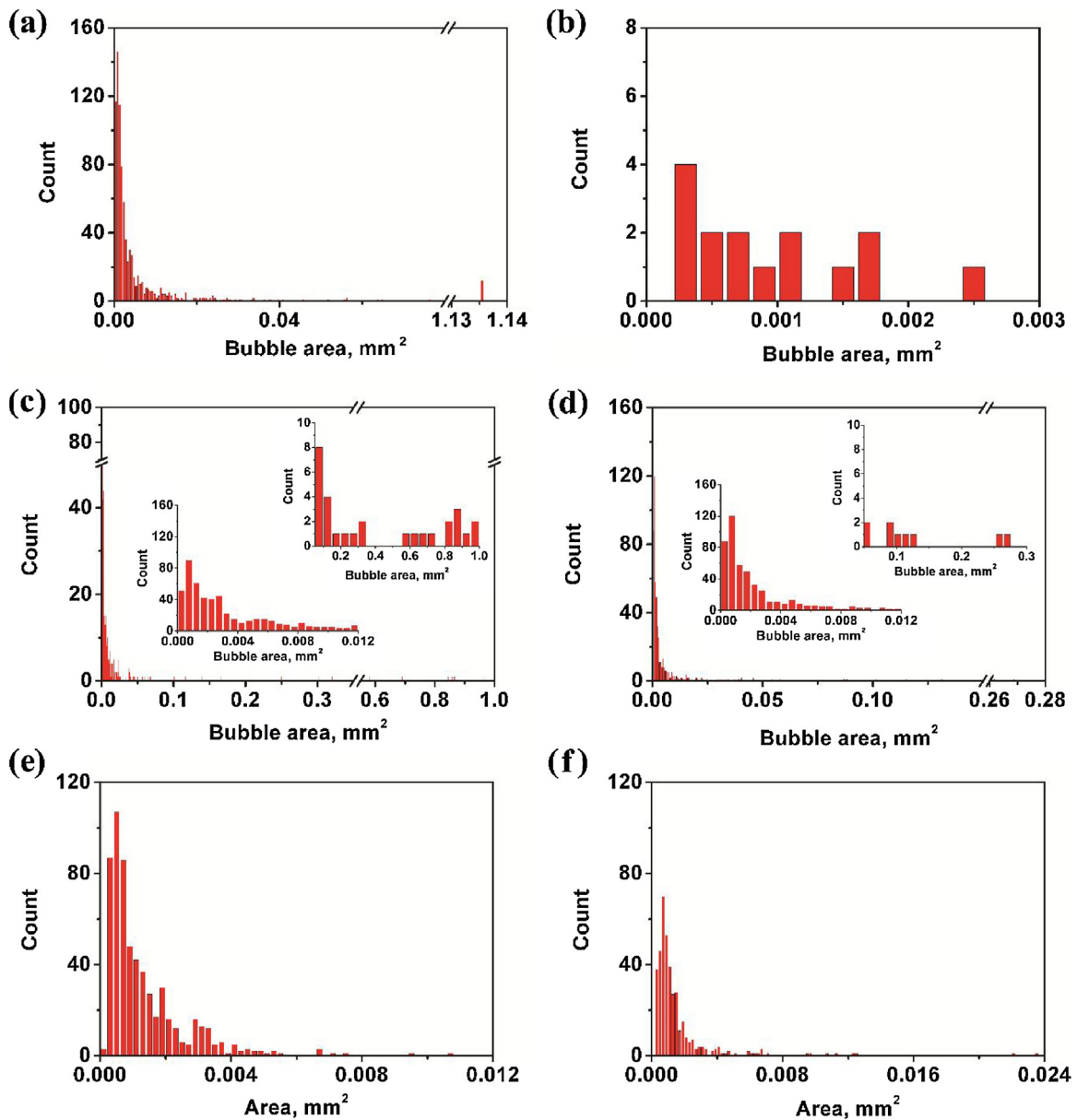


Fig. 10. Bubble size distribution comparison in (a)(c)(e) normal FLJ joints and (b)(d)(f) offset FLJ joints: bubble distribution observed from fracture surfaces on the CFRTP side for (a) normal FLJ and (b) offset FLJ at 600 rpm, (c) normal FLJ and (d) offset FLJ at 2000 rpm, with detailed bubble distribution inserted, and bubble distribution observed from cross-section of FLJ Cu/CFRTP joint for (e) normal FLJ and (f) offset FLJ at 1500 rpm.

Table 2

Bubble statistical results measured from cross sections of normal and offset Cu/CFRTP joints.

| Rotation rate, rpm | Normal FLJ | | | Offset FLJ | | |
|--------------------|------------|-------------------------------|---------------------------------|------------|-------------------------------|---------------------------------|
| | Number | Total area (mm ²) | Average size (mm ²) | Number | Total area (mm ²) | Average size (mm ²) |
| 600 | 46 | 0.23 | 0.0050 | 12 | 0.015 | 0.0012 |
| 800 | 4 | 0.06 | 0.0150 | 9 | 0.020 | 0.0022 |
| 1000 | 129 | 0.46 | 0.0036 | 37 | 0.190 | 0.0051 |
| 1500 | 601 | 0.80 | 0.0013 | 393 | 0.617 | 0.0016 |
| 2000 | 362 | 10.70 | 0.0296 | 69 | 0.150 | 0.0022 |

out. As a result, a high hardness because of the gathering of the carbon fibers exhibited in the center of the joint, with the typical microstructures shown in Fig. 12b.

At the edge, however, melted PA6 flowed in but carbon fibers was difficult to flow, and thus the CFRTP at the edge contained few carbon fibers, which reduced the strengthen effect of carbon fibers,

thereby reduced the CFRTP strength. Besides, the re-solidified plastic near the edge of the joint should be the first melted plastic flowing in, which experienced long time at high temperature to be decomposed. As a result, the degradation of the PA6 matrix largely increased, confirming by the over-melted yellow plastic in Fig. 3, which also probably largely reduce the CFRTP hardness [3]. There-

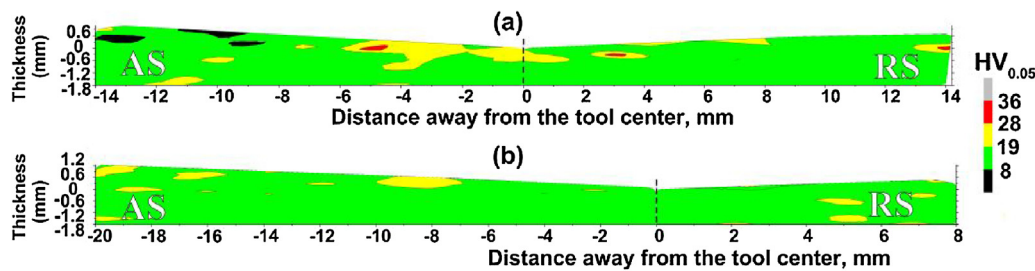


Fig. 11. Vickers hardness of CFRTM side near the interface of Cu/CFRTM joints at 2000 rpm for (a) normal, and (b) offset FLJ.

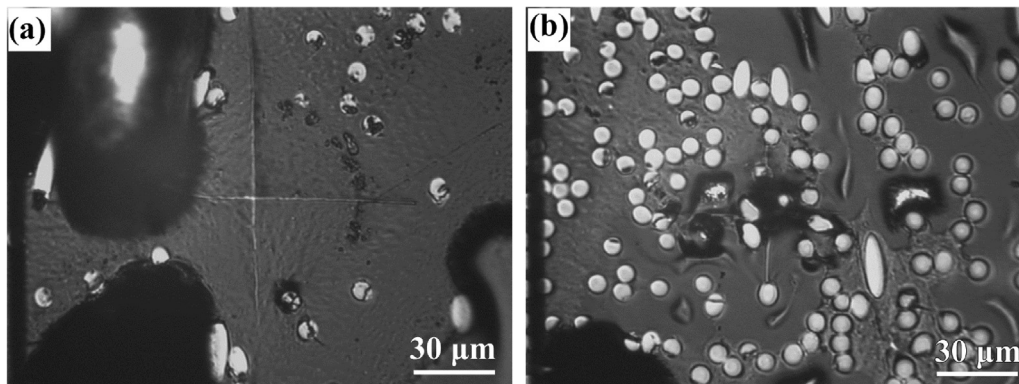


Fig. 12. Typical microstructure at CFRTM side with (a) low hardness on edge of the AS, and (b) high hardness near tool center line for normal FLJ joint at 2000 rpm.

fore, the low hardness zone was the result of large degradation, bubbles and few carbon fibers, with the typical microstructures shown in Fig. 12a.

Thus, local low hardness zone for the normal joints might become the fracture zone and reduce the joint strength. Compared to the normal joint, the offset joint experienced a shorter time for thermal decomposition of the plastic (Figs. 4 and 6c), reducing the degradation of PA6 matrix. Therefore, the less degradation of the CFRTM is another reason that tool offsetting enhanced the joint strength.

3.5. Main advantages of FLJ with tool offsetting

From the analysis above, the TSF increased after tool offsetting mainly because of three factors: the increase of the joining area, the decrease of the bubbles volume and the decrease of the CFRTM degradation. It was because tool offsetting could reduce the non-uniform temperature distribution in the joints, which resulted from the decrease of the cooling rate of the RS and the duration at the high temperature on the AS. It was reported that the bubbles are benefit for the bonding of plastics and metals during welding [4], while the bubbles remaining in the joints after welding reduced the joint strength. Therefore, the best way to obtain a sound joint with a high strength and the fewest bubbles is to produce enough pressure to make a strong bond by forming enough bubbles at a proper temperature during welding, and then expel these bubbles out of the joints. Tool offsetting might be an efficient way to achieve this goal for the FLJ of Cu to CFRTM. For example, in this study, the total area of bubbles at 800 rpm for the offset was very few (only 0.02 mm^2 , Table 2), accompanied by a high TSF of 3.37 kN (Fig. 6a). Although using some methods such as a silane coupling treatment on the surface of metals [18], the TSF of the metal/plastic joint can be enhanced, yet the total area of bubbles did not decrease. Therefore, tool offsetting can be a potential way to obtain an attractive set of properties for the FLJ of Cu to CFRTM.

4. Conclusion

In this study, Cu and CFRTM were successfully joined by FLJ with the tool in the joint center and offset the tool 7 mm toward the RS, respectively. The TSF of both the normal and offset joints first increased, and then decreased. Tool offsetting reduced the cooling rate on the RS, and thus reduced the non-uniform temperature distribution in the joints resulting from the high conductivity of Cu. This not only enhanced the TSF of the joints from 0.89–2.25 kN to 1.71–3.54 kN, with the maximum increasing rate of 135%, but also reduced the bubble area to only 19% of the original level of 2000 rpm. The large increase of the TSF after tool offsetting was attributed to the increase of the joining area, the decrease of the bubbles and the decrease of the CFRTM degradation. Tool offsetting is a good way to obtain a high-quality Cu/CFRTM joint with high strength and a low fraction of bubbles.

Conflicts of interest

The authors declare that they have no conflicts of interest.

References

- [1] C. Alia, J.M. Arenas, J.C. Suarez, R. Ocana, J.J. Narbon, J. Adhes. Sci. Technol. 27 (2013) 2480–2494.
- [2] A. Fink, P.P. Camanho, J.M. Andres, E. Pfeiffer, A. Obst, Compos. Sci. Technol. 70 (2010) 305–317.
- [3] K. Nagatsuka, S. Yoshida, A. Tsuchiya, K. Nakata, Compos. Part B 73 (2015) 82–88.
- [4] S. Katayama, Y. Kawahito, Scripta Mater. 59 (2008) 1247–1250.
- [5] K.W. Jung, Y. Kawahito, M. Takahashi, S. Katayama, Mater. Des. 47 (2013) 179–188.
- [6] S.T. Amancio, C. Bueno, J.F. dos Santos, N. Huber, E. Hage, Mater. Sci. Eng. A 528 (2011) 3841–3848.
- [7] G. Wagner, F. Balle, D. Eifler, Adv. Eng. Mater. 15 (2013) 792–803.
- [8] C. Engelmann, L. Oster, A. Olowinsky, A. Gillner, V. Mamuschkin, D. Arntz, J. Laser Appl. 29 (2017).
- [9] M. Wahba, Y. Kawahito, S. Katayama, J. Mater. Process. Technol. 211 (2011) 1166–1174.

- [10] K.W. Jung, Y. Kawahito, S. Katayama, *Sci. Technol. Weld. Join.* 16 (2011) 676–680.
- [11] K.W. Jung, Y. Kawahito, M. Takahashi, S. Katayama, *J. Laser Appl.* 25 (2013) 032003-6.
- [12] F.C. Liu, K. Nakata, J. Liao, S. Hirota, H. Fukui, *Sci. Technol. Weld. Join.* 19 (2014) 578–587.
- [13] F. Balle, S. Emrich, G. Wagner, D. Eifler, A. Brodyanski, M. Kopnarski, *Adv. Eng. Mater.* 15 (2013) 814–820.
- [14] L.H. Wu, D. Wang, B.L. Xiao, Z.Y. Ma, *Scripta Mater.* 78–79 (2014) 17–20.
- [15] R.S. Mishra, Z.Y. Ma, *Mater. Sci. Eng. R* 50 (2005) 1–78.
- [16] F.C. Liu, J. Liao, K. Nakata, *Mater. Des.* 54 (2014) 236–244.
- [17] K. Nagatsuka, D. Kitagawa, H. Yamaoka, K. Nakata, *ISIJ Int.* 56 (2016) 1226–1231.
- [18] K. Nagatsuka, H. Tanaka, B.L. Xiao, A. Tsuchiya, K. Nakata, Q. J. *Jpn. Weld. Soc. (in Japanese)* 33 (2015) 317–325.
- [19] F. Yusof, Y. Mutoh, Y. Miyashita, *Mater. Manuf. Technol.* 129–131 (2010) 714–718.
- [20] L.H. Wu, K. Nagatsuka, K. Nakata, *J. Mater. Sci. Technol.* 34 (2018) 192–197, <http://dx.doi.org/10.1016/j.jmst.2017.10.019>.
- [21] C.W. Chan, G.C. Smith, *Mater. Des.* 103 (2016) 278–292.
- [22] Y. Farazila, Y. Miyashita, W. Hua, Y. Mutoh, Y. Otsuka, *J. Laser Micro Nanoeng.* 6 (2011) 69–74.